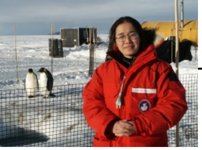

Lecture 27. Wind Lidar (6) Edge-Filter-Based Direct Detection Doppler Lidar

- FPI and Fizeau edge-filter DDL
- Iodine-absorption-line edge-filter DDL
- Edge-filter lidar data retrieval and error analysis
- Na-DEMOF DDL with multiple frequencies
- I_2-based Doppler lidar profiling of wind and temp
- Summary

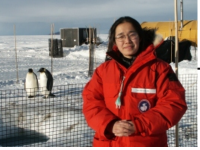

Direct Detection Doppler Lidar

- Direct detection Doppler lidars (DDL) convert the Doppler frequency shift to the change of intensity, or intensity ratio, or intensity spatial distribution for wind measurements.
- One of the key components for non-resonance DDL is the optical frequency discriminator or frequency analyzer, usually implemented in the lidar receiver if it is not available in the atmosphere.
- Current available optical frequency discriminators include

(1) Fringe imaging with optical interferometers (Fabry-Perot or Fizeau)
(2) Scanning FPI: tune the FPI peak transmission frequency
(3) Interferometer edge-filter: the edge of a transmission fringe of an optical interferometer (e.g., Fabry-Perot etalon or Fizeau etalon)
(4) Molecular absorption-line edge-filter (e.g., iodine I_2 absorption lines)
(5) Atomic absorption-line edge-filter (e.g., Na or K magneto-optic filter)
(6) Michelson or Mach-Zehnder interferometer with optical autocovariance

- A major difference between resonance DDL and non-resonance DDL lies in where the frequency discriminator is – in the atmosphere or in the receiver chain! Because the Fe Na, and K absorption lines are in the atmosphere, the lidar receiver is allowed to be broadband, rather than the narrowband employed in the non-resonance DDL.

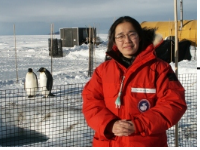

Edge-Filter DDL

- Edge filter is to use either high resolution Fabry-Perot etalons or atomic/molecular vapor cell filters to reject part of the return spectra while passing the other part of the spectra to two different channels. The wind or temperature information is then derived from the ratio of signals from these two channels.

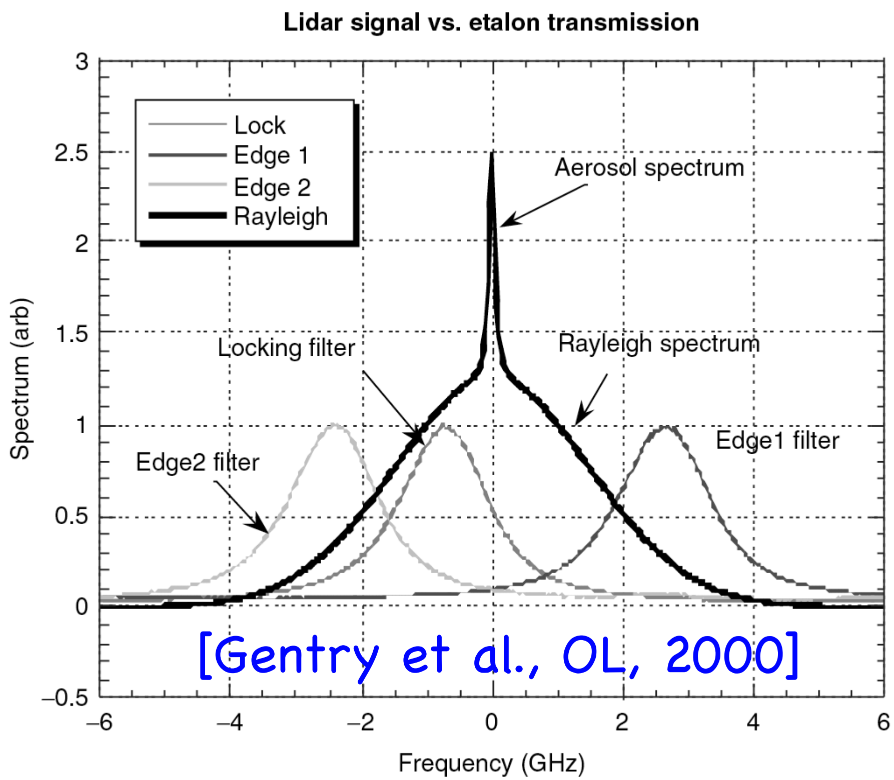

$$\frac{N_1}{N_2} = \frac{\xi_1 f_{m1}(T,P,V_R)}{\xi_2 f_{m2}(T,P,V_R)}$$

If V_R is known, then T can be derived.
If T is known, then V_R can be derived.

The locking filter channel is to ensure the optimum balance of the Edge 1 and Edge 2 filters (F-P etalons) on the zero Doppler-shifted laser signal.

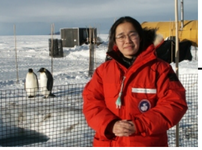

Single-Edge vs. Double-Edge

- Edge filter has single-edge and double-edge filters. See our textbook Chapter 7 “Wind Lidar” Direct-Detection Lidar.

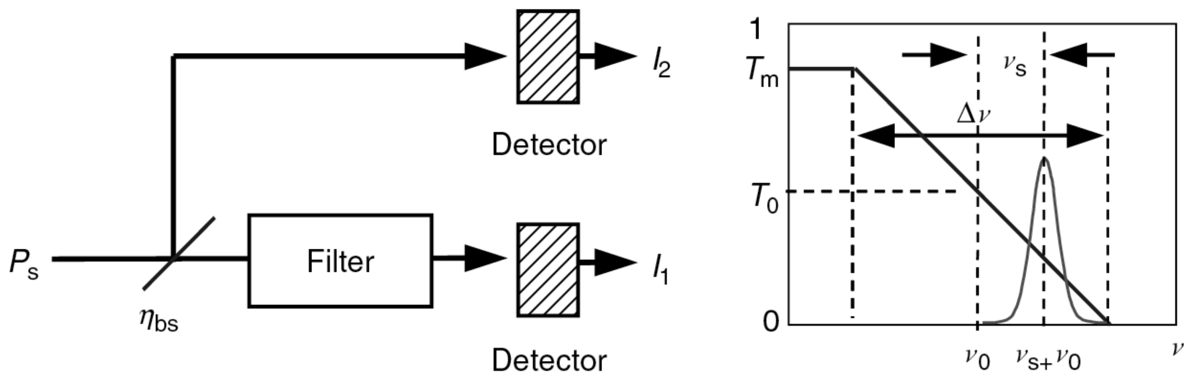

Figure 7.31 Single-edge functional diagram and filter transmission.

$$S = I_1/I_2 = \frac{\eta_{bs}}{(1-\eta_{bs})}\frac{\Re_1}{\Re_2}T_s$$
$$= \frac{\eta_{bs}}{(1-\eta_{bs})}\frac{\Re_1}{\Re_2}(T_0 - T_m\nu_s/\Delta\nu)$$

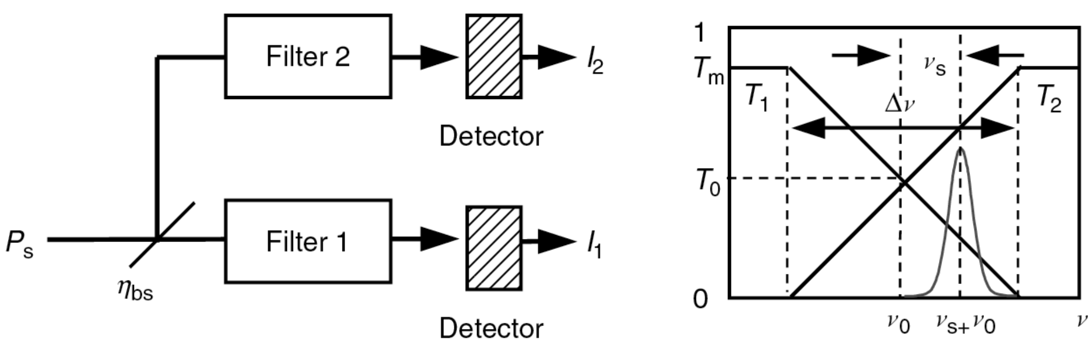

Figure 7.32 Double-edge functional diagram and filter transmission.

$$S = \frac{I_\Delta}{I_\Sigma} = \frac{I_1 - I_2}{I_1 + I_2} = \frac{T_{s_1} - T_{s_2}}{T_{s_1} + T_{s_2}} = \frac{2\nu_s}{\Delta\nu}$$

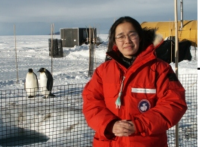

Freq Analyzer: Single-Edge Filter

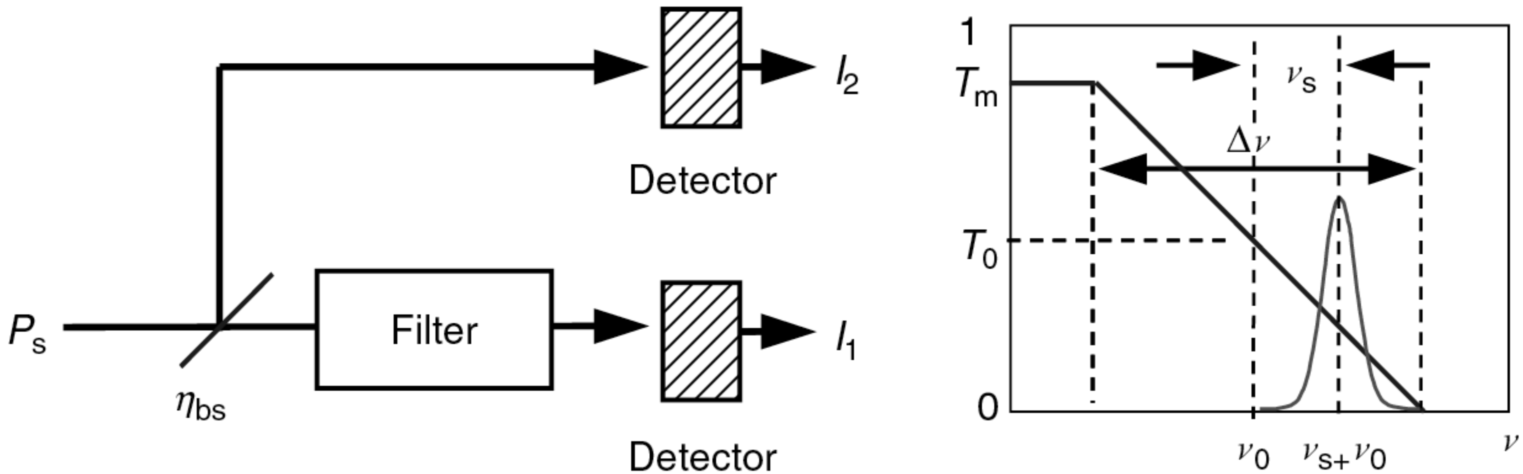

Figure 7.31 Single-edge functional diagram and filter transmission.

- A Fabry-Perot etalon is usually employed as the edge filter. The etalon is locked to the zero-Doppler laser frequency, ν_0, such that the frequency of the transmitted laser is matched to the mid-point of the quasi-linear transmission edge of the etalon.

- The intensity ratio of these two channels is a function of the Doppler frequency shift ν_s.

$$S = I_1/I_2 = \frac{\eta_{bs}}{(1-\eta_{bs})}\frac{\Re_1}{\Re_2}T_s$$

$$= \frac{\eta_{bs}}{(1-\eta_{bs})}\frac{\Re_1}{\Re_2}(T_0 - T_m\nu_s/\Delta\nu)$$

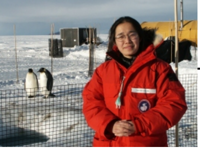

Freq Analyzer: Double-Edge Filter

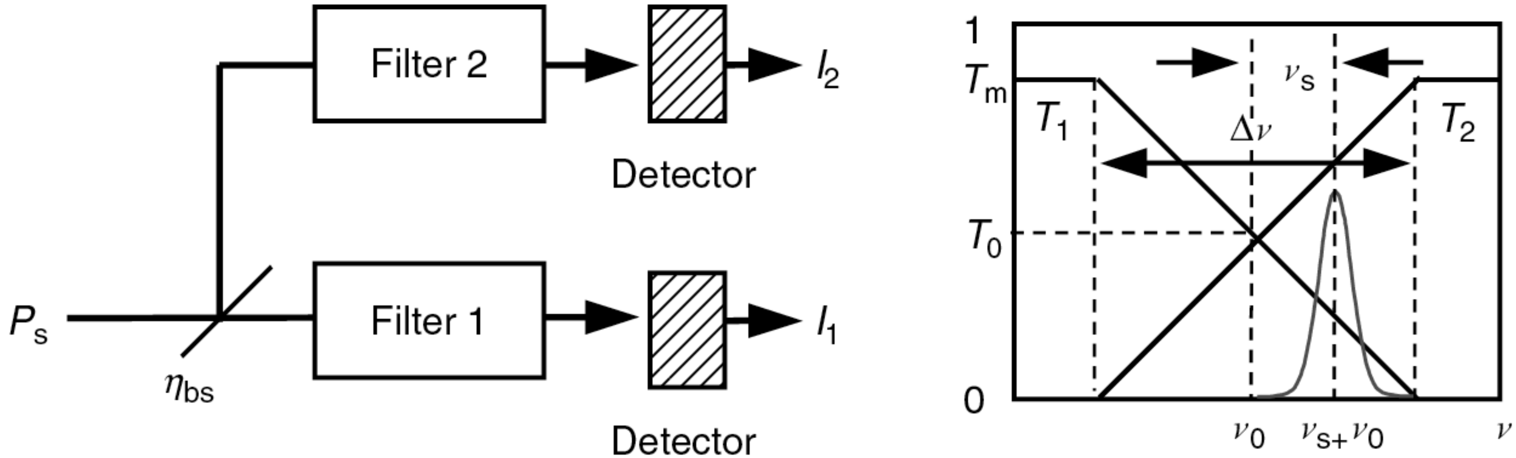

Figure 7.32 Double-edge functional diagram and filter transmission.

- ❑ Two oppositely sloped quasi-linear discriminator edges are used for the two receiver channels in the double-edge design. Usually etalon transmission fringes are used to create the edges. The etalons are locked together (mid-point) to the zero-Doppler transmitted laser frequency ν_0.

- ❑ The intensity ratio of the difference between the two signals to the sum is a sensitive function of the Doppler frequency shift ν_s.

$$S = \frac{I_\Delta}{I_\Sigma} = \frac{I_1 - I_2}{I_1 + I_2} = \frac{T_{s_1} - T_{s_2}}{T_{s_1} + T_{s_2}} = \frac{2\nu_s}{\Delta\nu}$$

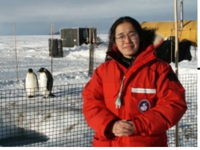

Detectors for FPI Edge-Filter DDL

- The information presented to the detector in an edge detection system is the image of the small on-axis solid angle corresponding to the central on-axis fringe of the Fabry-Perot etalon with the necessary spectral FWHM. A suitable detector will be one that has high quantum efficiency, low noise, the capability for photon counting or analog read-out, depending on the intensity of the signal, and which can be "time-gated" to provide range-resolved information.
- The conventional PMT, the APD, and the CCD are among several that have been used successfully, depending on the spectral region of the wind lidar. The PMT is a device that is essentially noise-free when used in photon-counting mode. Due to the negligible read-out and electronic noise, the PMT signal may be post-integrated with complete flexibility, leading to the PMT being widely used as a detector of choice, particularly at 355 and 532 nm. Its drawback is the modest quantum efficiency of the photocathode of the device, normally limited to values of order 40% or less, depending on the spectral region.
- 2-D detection: altitude range and time, similar to other lidars, except the fringe-imaging lidars.

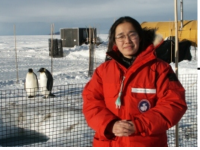

Fringe Imaging vs Edge Filters

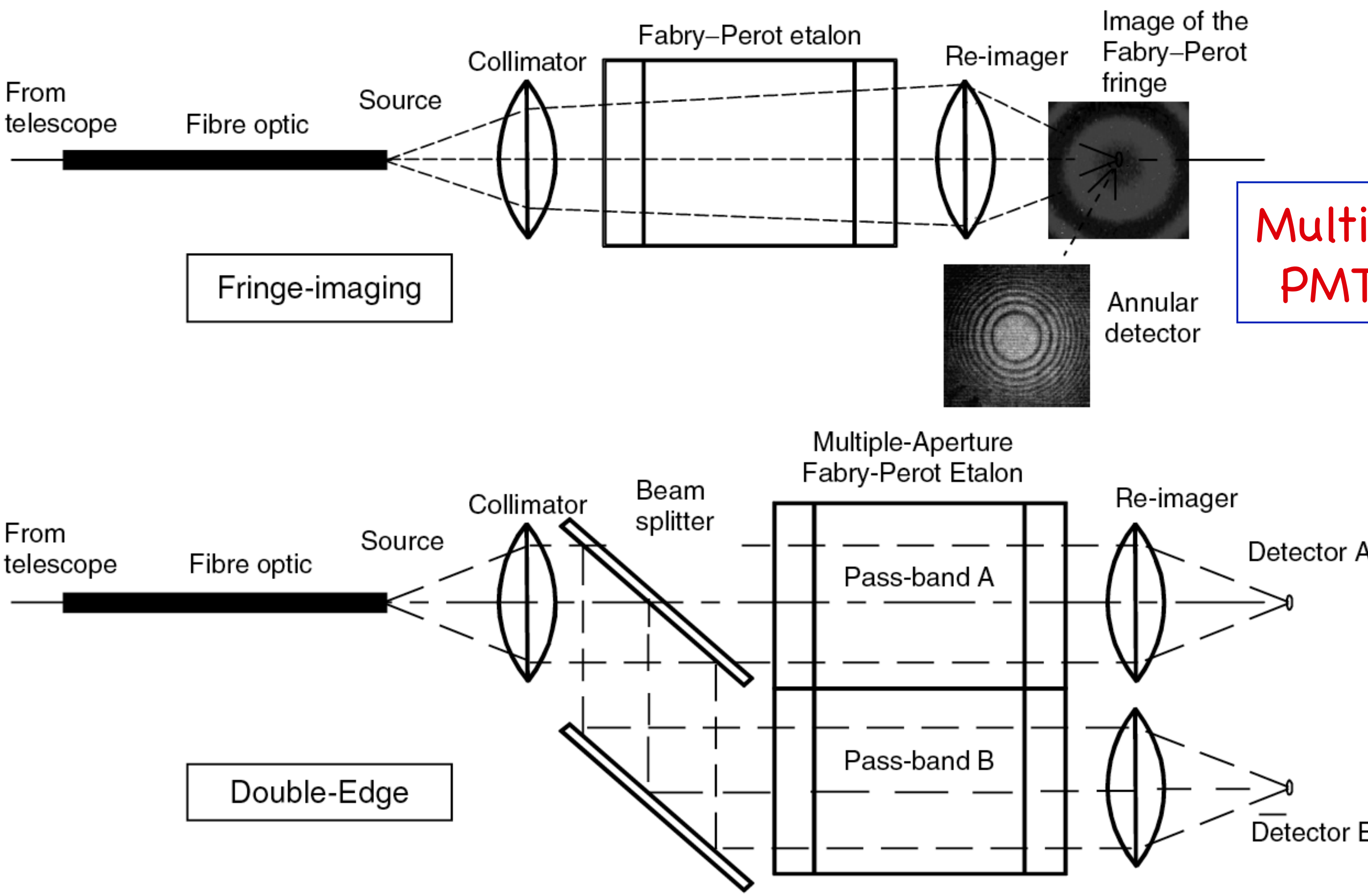

Multi-Channel PMT or CCD

PMT
APD
CCD

Figure 7.45 The fringe-imaging and double-edge detection methods for direct detection are shown conceptually.

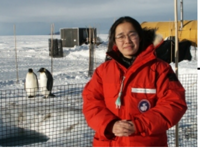

DDL Based on Fizeau Etalon

- DDL based on Fizeau interferometer: linear fringes.

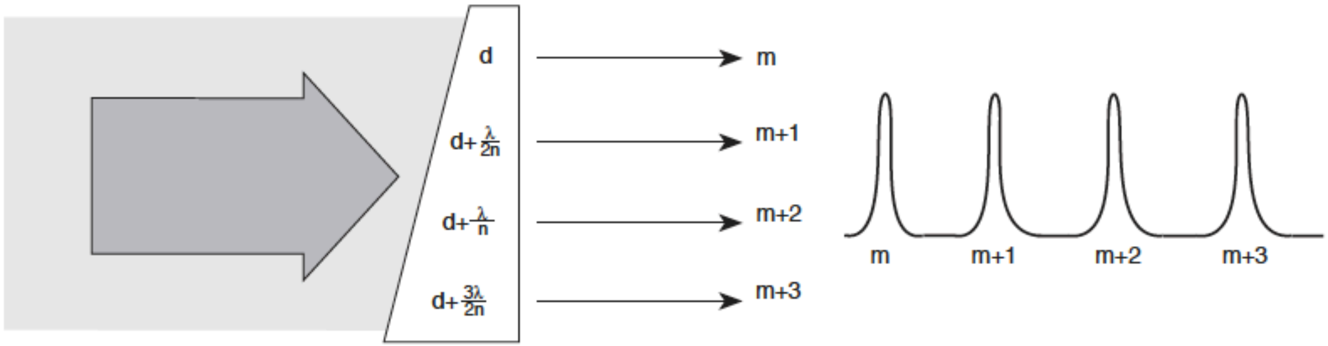

Fizeau etalon

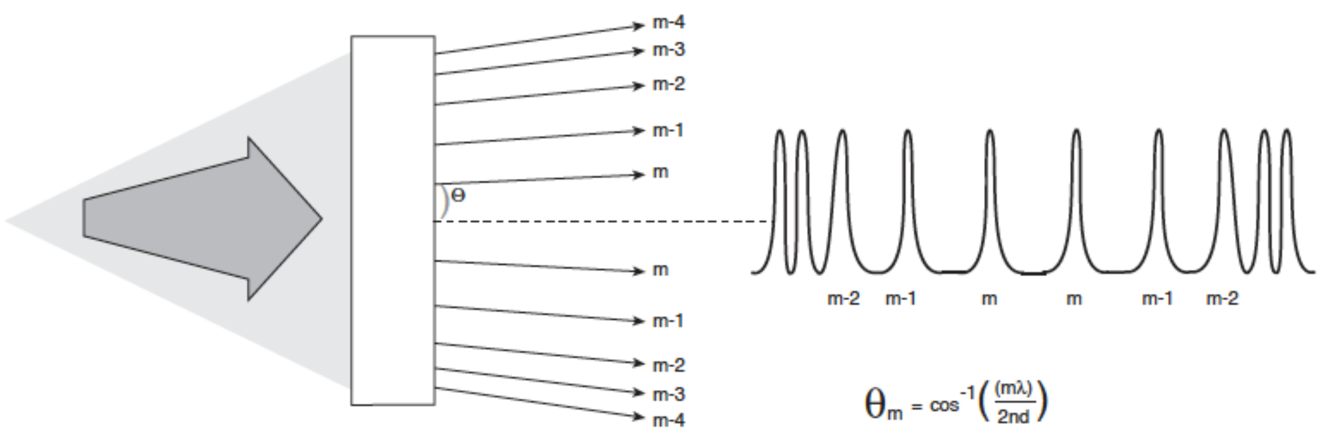

Fabry-Perot etalon

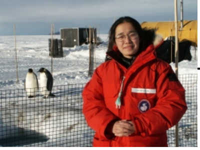

I_2 Absorption Lines Edge-Filter DDL

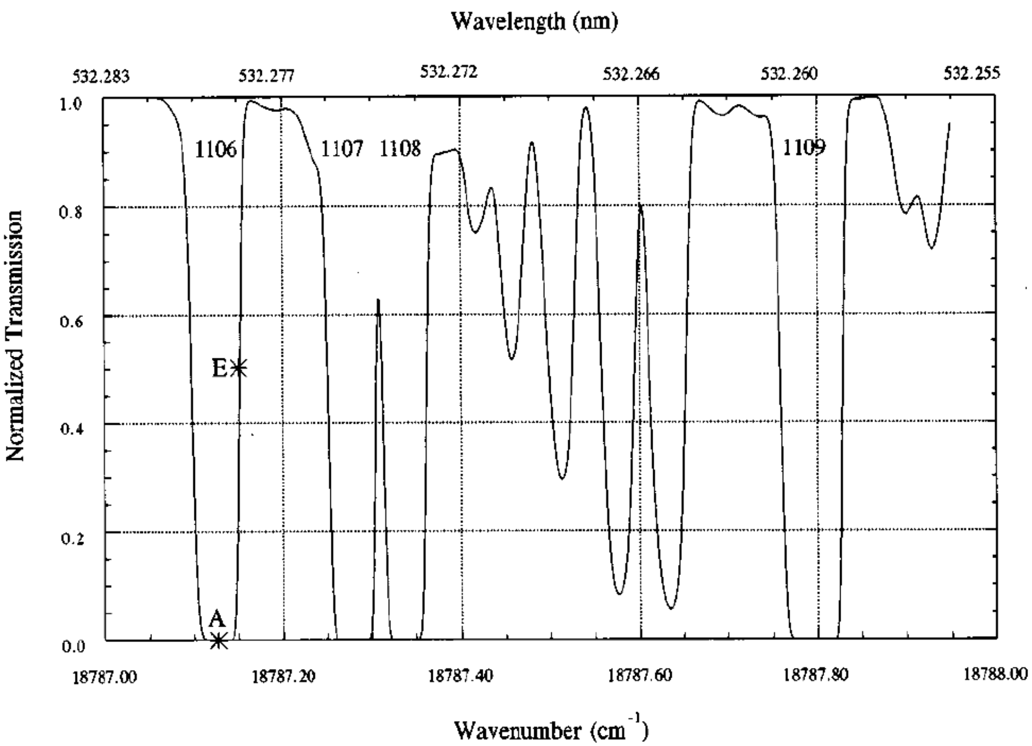

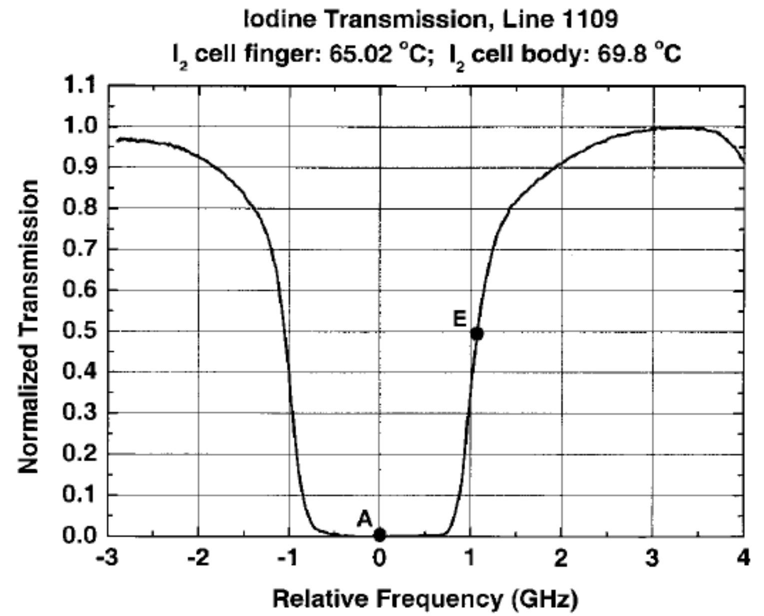

Fig. 2. Normalized transmission for absorption line 1109 of the iodine filter near 532 nm. The temperature of cell finger and cell body are 65.02 °C and 69.8 °C, respectively. The wave numbers at reference point A and locking point E are 18787.796 and 18787.830 cm^{-1} (1.02 GHz apart), respectively.

[Liu et al., Appl. Phys. B 64, 561-566, 1997]
[Friedman et al., Opt. Lett., 22, 1648-1650, 1997]
[Liu et al., Appl. Opt., 41, 7079-7086, 2002]
[Wang et al., Applied Optics, 49, 6960-6978, 2010]

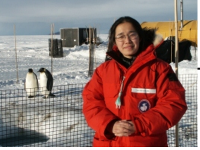

Iodine-filter-based Doppler Lidar

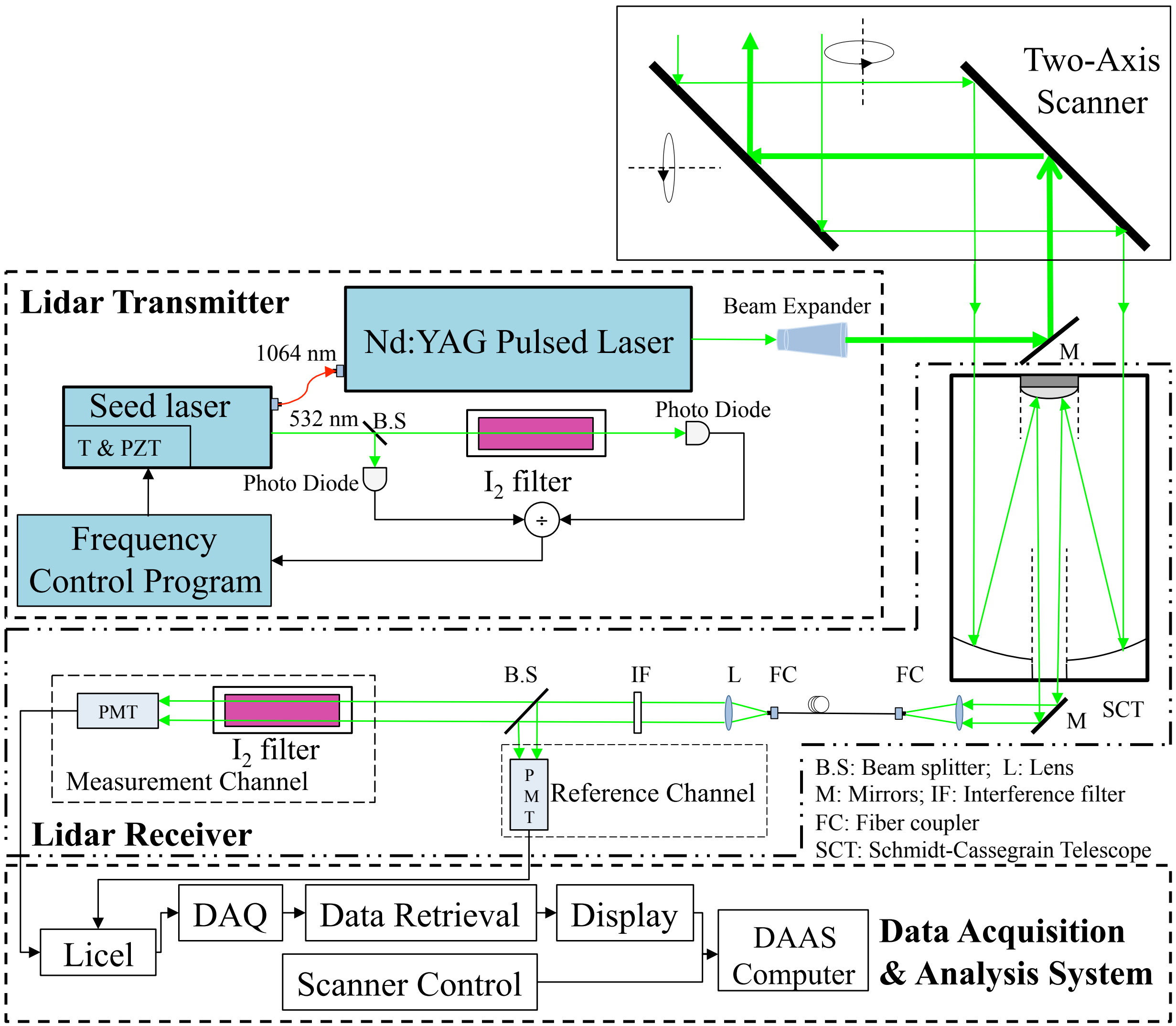

[Wang et al., Applied Optics, 49, 6960-6978, 2010]

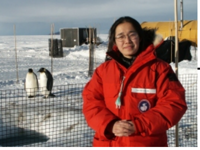

Wind Measurements by I_2 Doppler Lidar

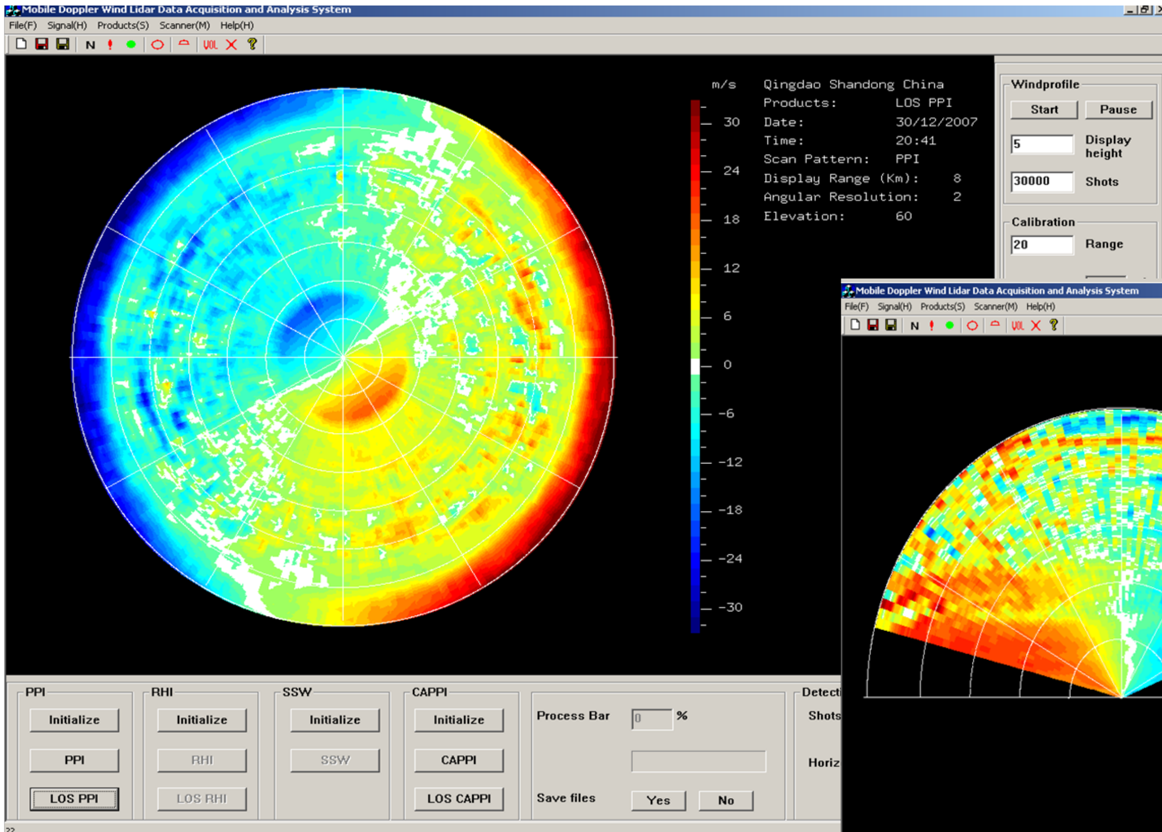

RHI scan

(Range Height Indicator)

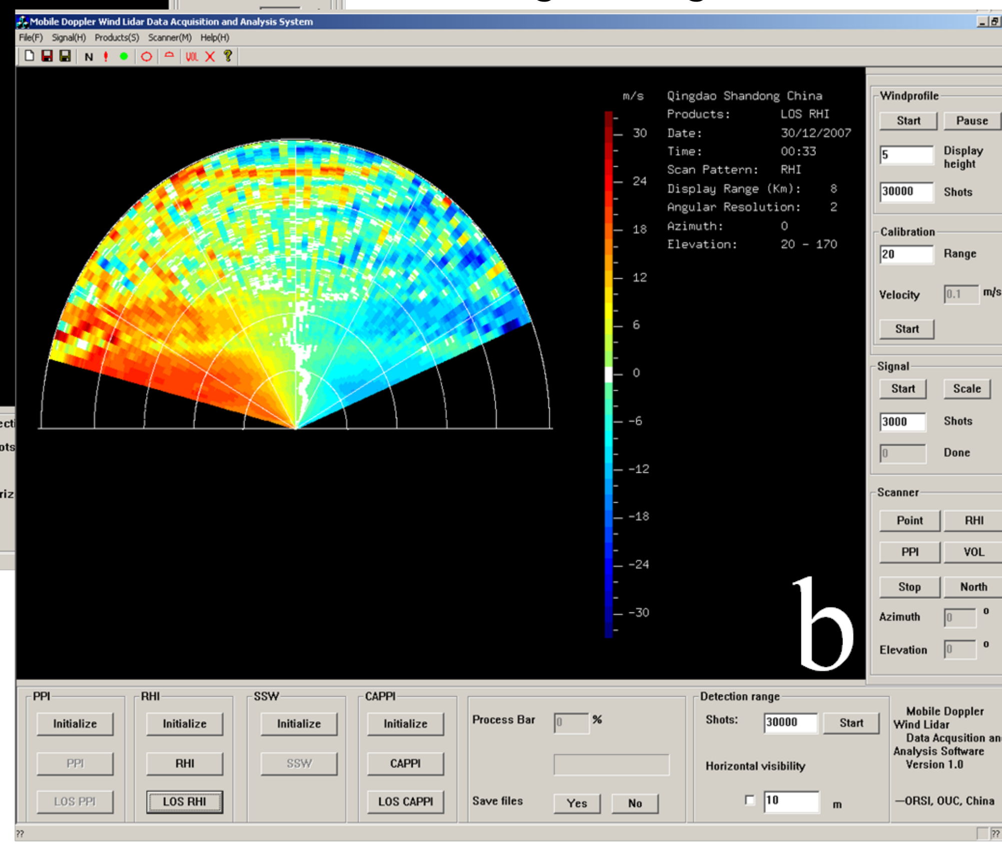

PPI scan

(Plan Position Indicator)

[Wang et al., Applied Optics, 49, 6960-6978, 2010]

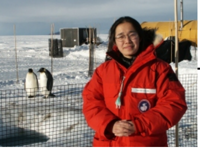

DDL Data Retrieval and Error Analysis

$$V_{\mathrm{LOS}} = 0 + V_{\mathrm{LOS},H} + V_{\mathrm{LOS},V}, \tag{1}$$

where 0 represents zero LOS wind, $V_{\mathrm{LOS},H}$ and $V_{\mathrm{LOS},V}$ are the horizontal and vertical wind components to the LOS direction. Positive LOS wind velocity is defined as radially outward from the lidar. We define $R_{W,i}$ as the wind ratio of signal photon counts of the measurement channel to the reference channel in the ith (azimuth) LOS direction, which contains the information of Doppler shift. Using a linear approximation that the wind ratio after normalization to the zero-wind ratio is linearly proportional to the LOS wind velocity, we can express the overall wind ratio $R_{W,i}$ by

$$R_{W,i} = R_0 - \Delta R_{H,i} - \Delta R_{V,i}, \tag{2}$$

where R_0 is the zero-wind ratio corresponding to the "0" written in Eq. (1), i.e., the ratio of the measurement channel to the reference channel when the LOS wind velocity is zero, and $\Delta R_{H,i}$ and $\Delta R_{V,i}$ are the wind ratio changes caused by the horizontal and vertical wind components in the ith LOS direction,

Under such linear approximation, we have the relationship

$$\Delta V_{\mathrm{LOS}} = \frac{dV_{\mathrm{LOS}}}{dR_W}\Delta R_W, \tag{3}$$

where $\Delta V_{\mathrm{LOS}} = V_{\mathrm{LOS}} - 0$ and $\Delta R_W = R_W - R_0$. Therefore, the LOS wind velocity can be calculated from the measured wind ratios using

$$V_{\mathrm{LOS},i} = \frac{R_{W,i} - R_0}{R_0 S}, \tag{4}$$

where $R_{W,i}/R_0$ is the normalized wind ratio as defined in [18], and S is the wind measurement sensitivity. The sensitivity S is defined as the fractional change in the wind ratio per unit change in LOS wind velocity

$$S = \frac{1}{R_0}\frac{dR_W}{dV_{\mathrm{LOS}}} = 3.76^* \frac{1}{R_0}\frac{dR_W}{d\nu}, \tag{5}$$

where ν is the laser frequency and 3.76 MHz/(m/s) is the Doppler shift of backscattered light caused by 1 m/s LOS wind velocity, which is given by $2/\lambda = 2/532$ nm. Here $\lambda = 532$ nm is the outgoing laser wavelength. Therefore, after S is derived from

[Wang et al., Applied Optics, 49, 6960-6978, 2010]

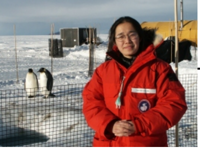

DDL Data Retrieval and Error Analysis

the experimentally measured $\frac{dR_W}{d\nu}$ and R_0, we can calculate the LOS wind velocity as follows:

$$V_{\mathrm{LOS},i} = \frac{R_{W,i} - R_0}{3.76^* dR_W/d\nu}. \qquad (6)$$

Equation (6) is the basic relationship used in the derivation of the LOS wind velocity. Besides the measured wind ratio $R_{W,i}$, the fidelity of this data retrieval method relies on how well the two parameters R_0 and $\mathrm{d}R_W/\mathrm{d}\nu$ can be determined experimentally. To do so, two assumptions are further made in addition to the spatial homogeneity assumption mentioned earlier. First, the vertical wind assumption—the vertical wind averaged over sufficient periods is close to zero. Second, the uniform sensitivity assumption—the slope $\mathrm{d}R_W/\mathrm{d}\nu$ remains constant from the zenith to the off-zenith directions within a short measurement period and over a small scanned volume. Any deviation of the assumptions from the actual atmosphere conditions will lead to systematic errors in the retrieved LOS wind. The error analysis provided

Universal and robust error-analysis

$$\Delta V_{\mathrm{LOS}} = \frac{\partial V_{\mathrm{LOS}}}{\partial R_W}\Delta R_W + \frac{\partial V_{\mathrm{LOS}}}{\partial R_0}\Delta R_0 + \frac{\partial V_{\mathrm{LOS}}}{\partial (dR_W/d\nu)}\Delta(dR_W/d\nu), \qquad (19)$$

where ΔR_W, ΔR_0, and $\Delta(dR_W/d\nu)$ represent the errors in the corresponding measured parameters, respectively. As the three error terms are not correlated and the partial derivatives on the right side of Eq. (19) can be easily derived from Eq. (6), the total root mean square (rms) LOS wind error is given by the error propagation

$$(\Delta V_{\mathrm{LOS}})_{\mathrm{rms}} = \frac{1}{3.76^*(dR_W/d\nu)} \times \sqrt{(\Delta R_W)^2 + (\Delta R_0)^2 + [3.76 V_{\mathrm{LOS}}\Delta(dR_W/d\nu)]^2}, \qquad (20)$$

[Wang et al., Applied Optics, 49, 6960-6978, 2010]

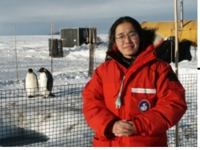

DDL Data Retrieval and Error Analysis

The sources of errors can be classified into two categories. One is the uncertainties in measured R_W, R_0, and $dR_W/d\nu$, mainly resulting from the photon noise of the return signals. The errors caused by these uncertainties are termed the "precision of wind measurements," and are random errors. The other source is the biases, mainly caused by the deviations of our assumptions from the actual meteorological conditions in our case. The resulting errors are termed the "accuracy of measurements," and are systematic errors. Here we discuss the precision and accuracy, respectively, of the lidar wind measurements.

With respect to the measurement precision, the photon-noise-induced random errors are estimated below for R_W, R_0, and $dR_W/d\nu$. The wind ratio is given by $R_W = N_M/N_R$, where N_M and N_R are the signal photon counts of the measurement and reference channels, respectively. Following the derivation in [5] for photon noise and recognizing that the photon counts obey a Poisson distribution, the rms error of the wind ratio R_W is given by

$$\left(\frac{\Delta R_W}{R_W}\right)_{\text{rms}} = \frac{\sqrt{1+\frac{1}{R_W}}}{\sqrt{N_R}}\sqrt{1+\frac{2B_M+\frac{2B_R}{R_W^2}}{N_R\left(1+\frac{1}{R_W}\right)}}, \quad (21)$$

$$(\Delta V_{\text{LOS}})_{\text{rms}} = \frac{\sqrt{2}\cdot(\Delta R_W)_{\text{rms}}}{3.76^*(dR_W/d\nu)} \approx \frac{\sqrt{2}}{S}\cdot\left(\frac{\Delta R_W}{R_W}\right)_{\text{rms}}. \quad (22)$$

For the data retrieval methods described in Subsection 4.A, R_0 and $dR_W/d\nu$ are two parameters that must be determined experimentally under three assumptions (the horizontal homogeneity of atmosphere, the zero vertical wind, and the uniform sensitivity assumptions) mentioned above. Any deviations of the assumptions from the actual atmospheric conditions will result in bias in the measured R_0, and $dR_W/d\nu$, thus affecting the accuracy of LOS wind retrieval. We examine the roles of these two terms in the

$$\Delta V_{\text{LOS}} = V_{\text{LOS}}\frac{\Delta(dR_W/d\nu)}{(dR_W/d\nu)}, \quad (23)$$

$$\Delta V_{\text{LOS}} = \frac{\Delta R_0}{3.76^*(dR_W/d\nu)} = \frac{1}{S}\cdot\frac{\Delta R_0}{R_0}, \quad (24)$$

[Wang et al., Applied Optics, 49, 6960-6978, 2010]

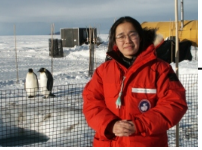

DDL Data Retrieval and Error Analysis

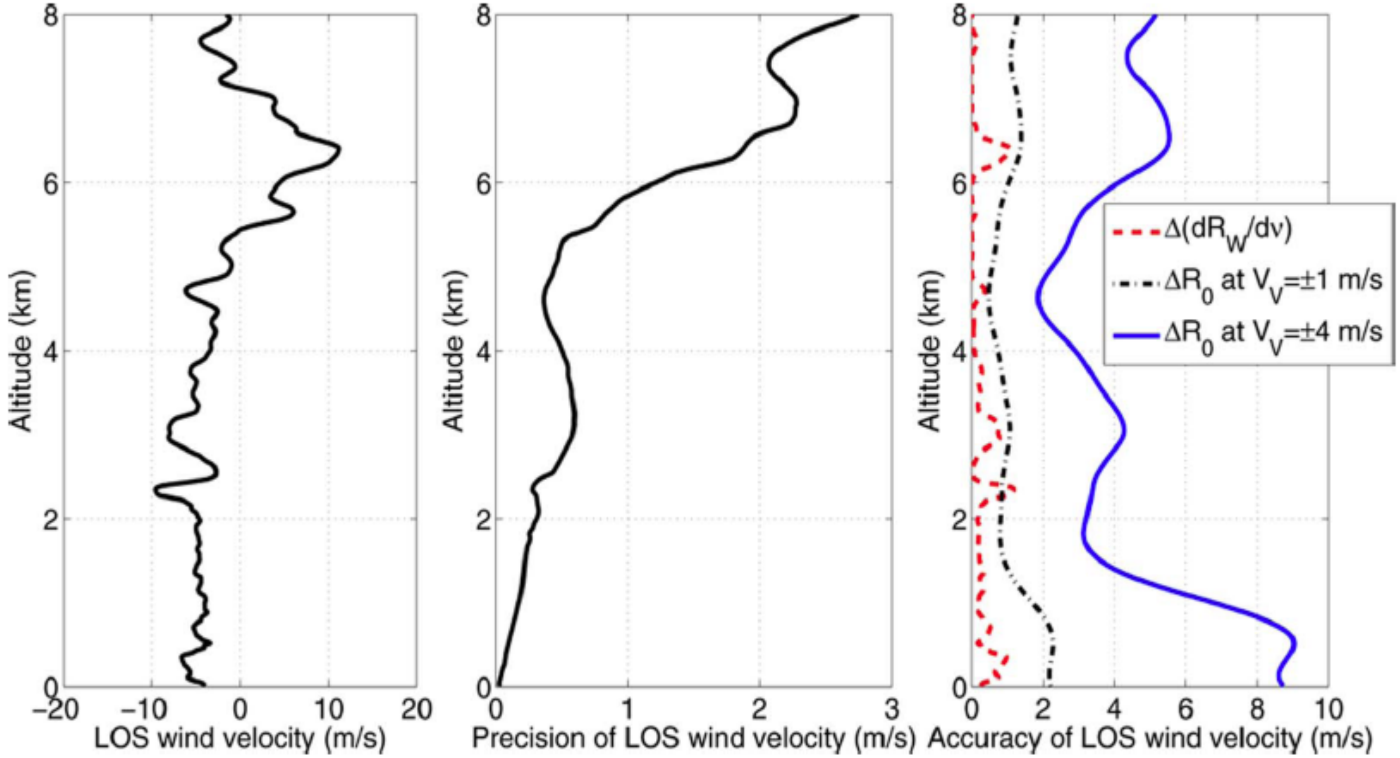

Fig. 8. (Color online) LOS wind velocity measured at azimuth of 90° (east) by the Doppler lidar at 22:09 LT on 4 March 2008, and the wind uncertainty under different vertical winds. The integration time $\Delta t = 100$ s and the spatial resolution $\Delta z = 10$ m.

[Wang et al., Applied Optics, 49, 6960-6978, 2010]

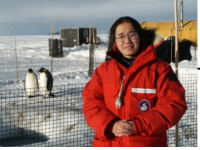

Assumptions in Edge-Filter DDL

- To derive wind from edge-filter DDL, several quantities have to be taken from models or from independent measurements.

- Temperature profile: since the Doppler broadening (depending on temperature) affects the transmitted signal strength, it has to be pre-determined or taken from models for single or double-edge filters.

- Aerosol-scattering ratio also has to be determined independently when in the atmosphere region with aerosols. For example, in the I_2 filter case, tuning the Nd:YAG laser to point A can eliminate aerosol signal thus deriving the aerosol scattering ratio when combined with the reference channel.

- Background counts in each channel.

- Of course, filter transmission functions have to be known and determined to high precision and accuracy.

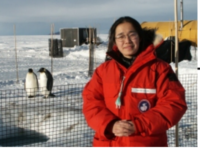

Considerations for DDL

- Precision requirement: for δV = 1 m/s velocity precision, the freq measurement precision required for the optical freq analyzer in a DDL is $\delta\nu = 2(\delta V)/\lambda$ = 5.6 MHz for 355 nm.

- Accuracy requirement: accuracy should surpass the precision level. This is usually achieved by monitoring the transmitted laser pulse signal or alternatively measuring the backscatter signal from a stationary or very low velocity target or lock the laser and the filter transmission to each other.

- Calibration or accuracy is a main problem for non-resonance DDL, because the burden is on the receiver chain which is variable through time or surrounding conditions, especially in FPI case.

- On the other hand, resonance fluorescence Doppler lidars put the discriminator to the atomic absorption lines, which do not change with time. Their receivers can be much simpler.

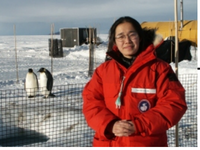

Papers on DDL wind measurements with a Cabannes-Mie lidar

- She et al., Appl. Opt., 46, 4434-4443, 2007: Comparison between iodine vapor filter and FPI
- She et al., Appl. Opt., 46, 4444-4454, 2007: impact of aerosol variations on the iodine filter methods
- There are several classic papers on the edge filter techniques providing good insight of the DDL techniques:
  - C. L.Korb, Bruce M. G. and C. Y. Weng, Edge technique: theory and application to the lidar measurement of atmosphere wind, Appl. Opt., **31**, 4202-4212, (1992).
  - M. L. Chanin, A. Hauchecorne, A. Garnier and D. Nedeljkovic, Recent lidar developments to monitor stratosphere-troposphere exchange, J. Atom. Sol. Terr. Phys., **56**, 1073-1081 (1994).
  - C. Flesia and C. L. Korb, Theory of the double-edge molecular technique for Doppler lidar wind measurement, Appl. Opt., **38**, 432-440 (1999).
  - J. McKay, Assessment of a multibeam Fizeau wedge interferometer for Doppler wind lidar, Appl. Opt. **41**, 1760-1767 (2002).

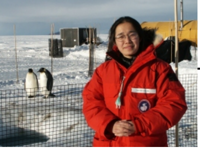

Multiple-Frequency Na/K Double-Edge Magneto-Optic Filter DDL

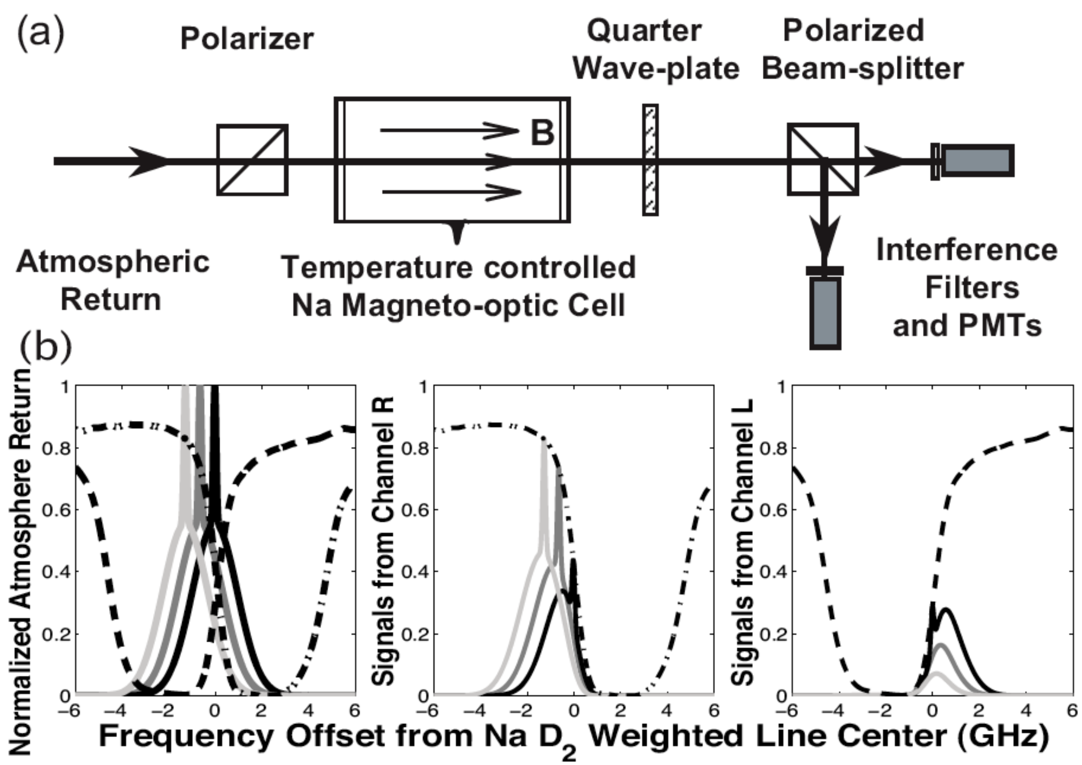

Na Double-Edge Magneto-Optic Filter (Na-DEMOF)

- With a 3-freq Na or K Doppler lidar, it is possible to measure wind, temperature, and aerosol simultaneously with a Na-DEMOF or K-DEMOF.

[Huang, Chu, Williams, et al., Optics Letters, 34, pp.199, 2009]

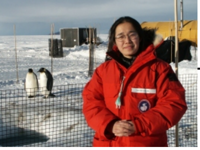

DEMOF with a 3-freq Na Doppler Lidar

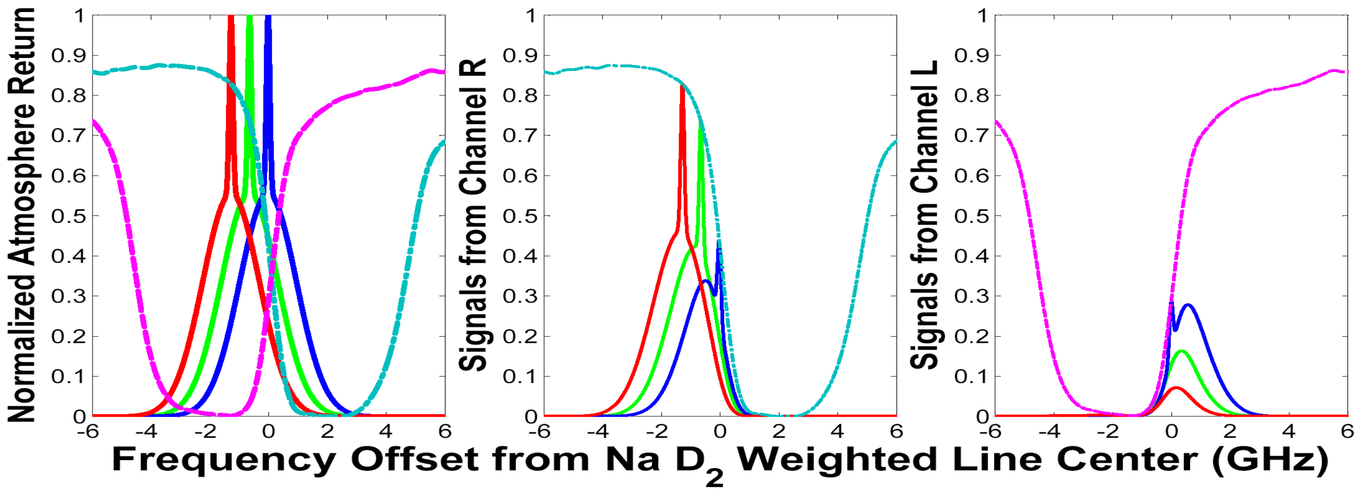

Calibration curves for ratio technique with Na-DEMOF

$$R_W(V_{LOS},T,R_b)=\frac{N_{R+}-N_{L+}}{N_{R+}+N_{L+}}$$

$$R_T(V_{LOS},T,R_b)=\frac{N_{L-}}{N_{R-}}$$

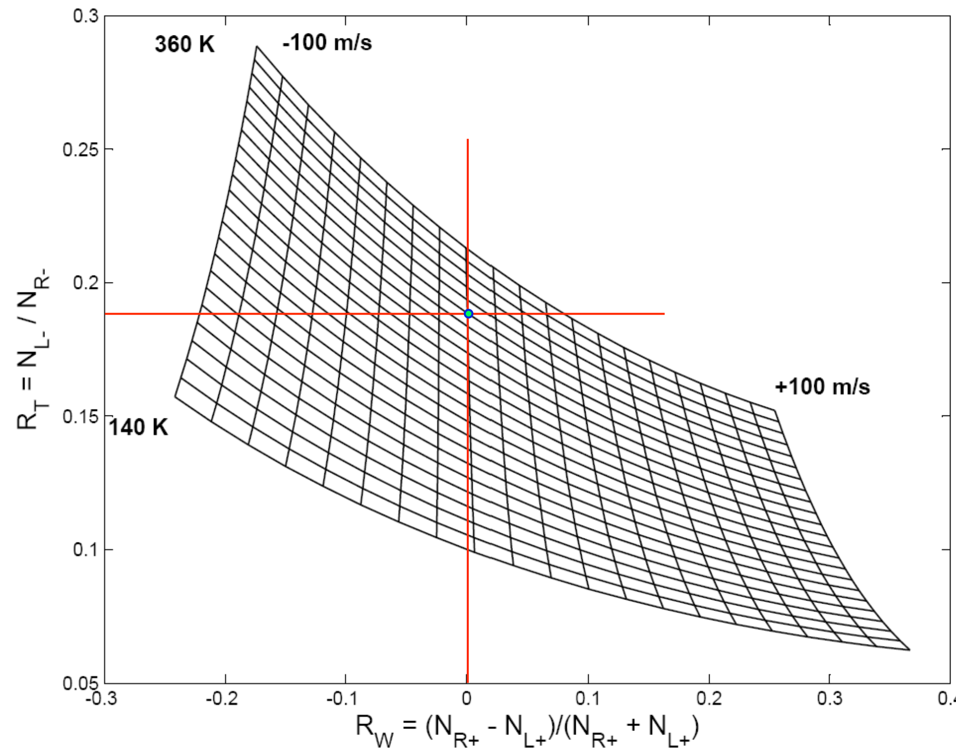

- Temperature and wind are determined simultaneously from two ratios.

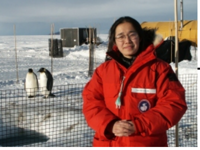

Field Demonstration of Simultaneous Wind and Temperature Measurements (10-45 km) with Na-DEMOF and 3-Frequency Na Lidar

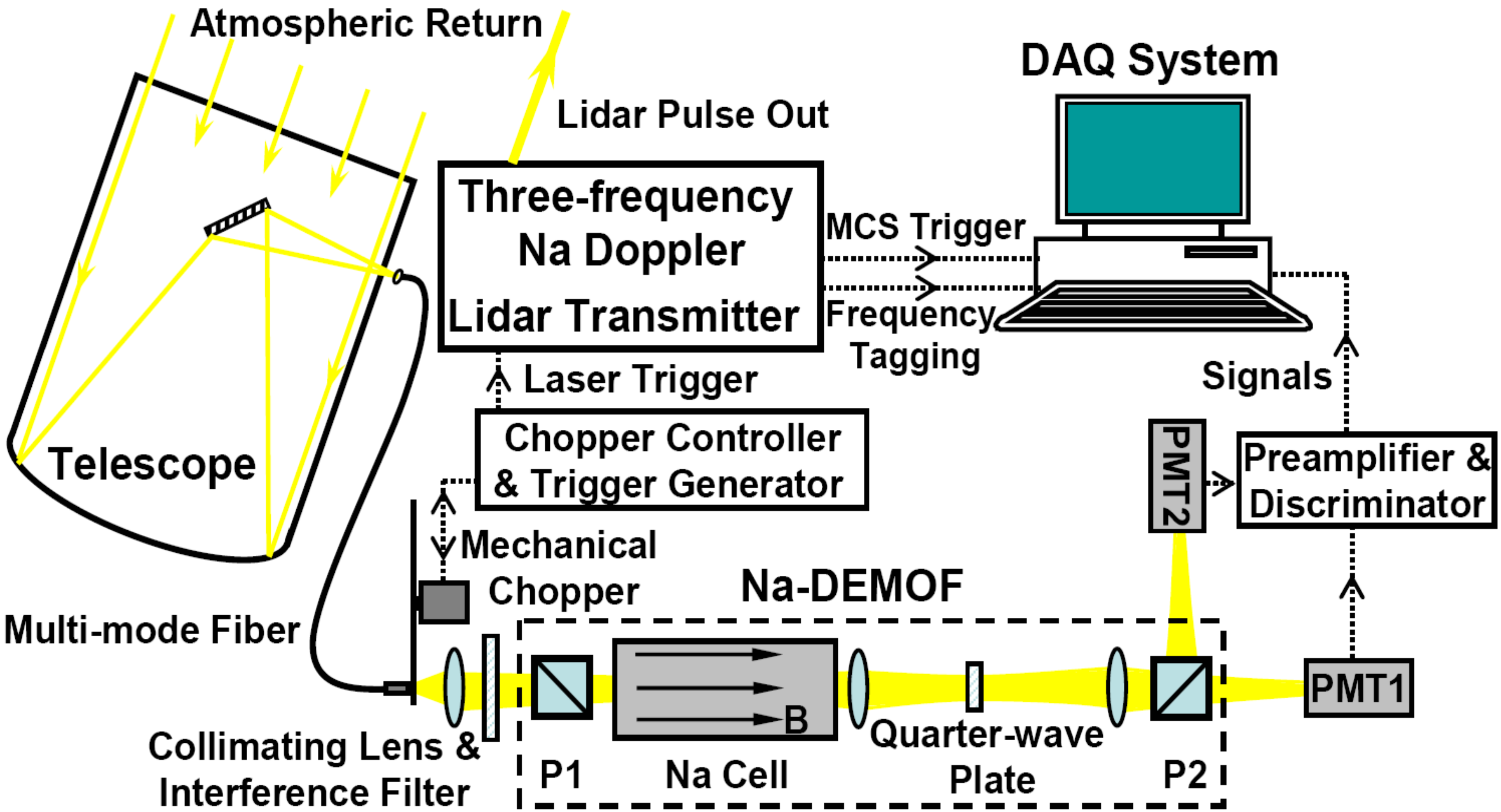

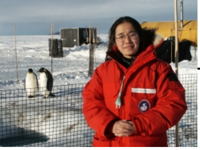

Field Demonstration of Simultaneous Wind and Temperature Measurements (10-45 km) with Na-DEMOF and 3-Frequency Na Lidar

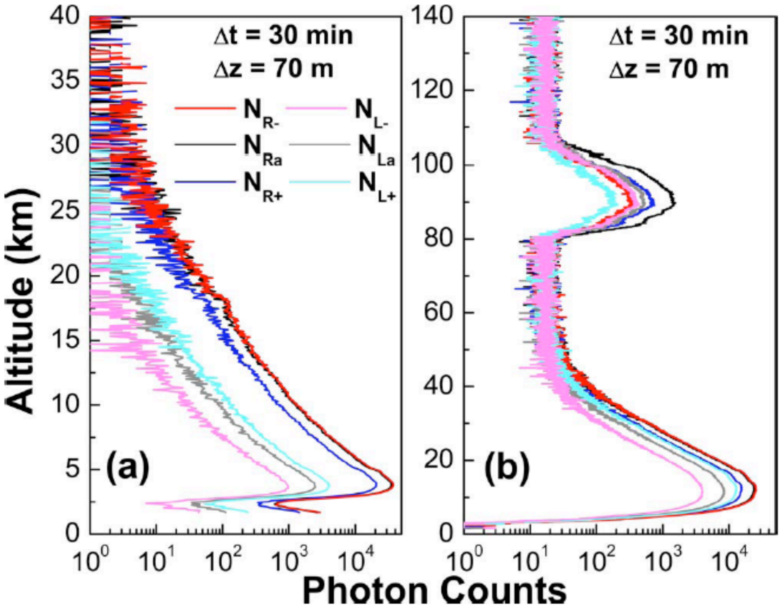

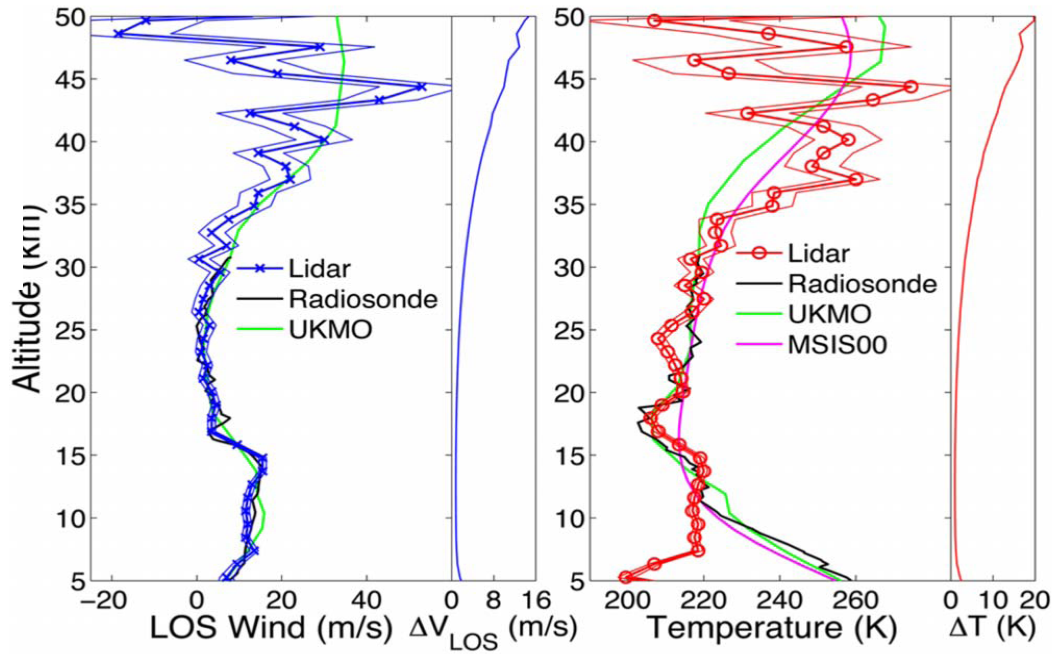

[Huang, Chu, et al., Optics Letters, 34, pp. 1552, 2009]

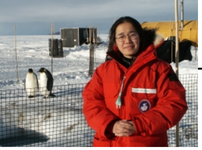

Doppler Rayleigh Iodine Spectrometer-Based Doppler Rayleigh/Mie/Raman Lidar to Profile Wind and Temperature up to 80 km

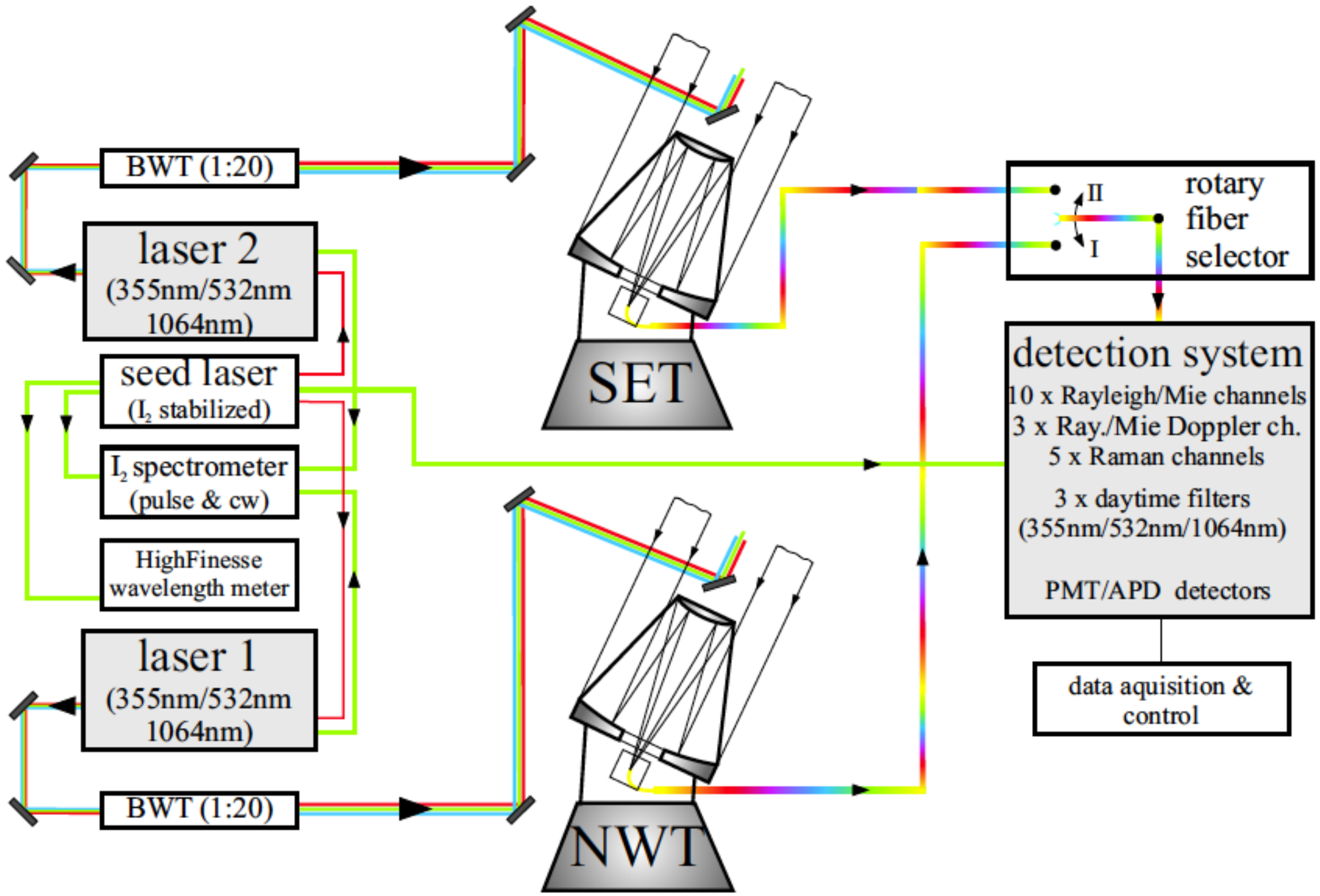

[Baumgarten, Atmos. Meas. Tech., 3, 1509-1518, 2010]

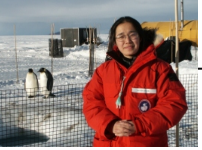

Doppler Rayleigh Iodine Spectrometer-Based Doppler Rayleigh/Mie/Raman Lidar to Profile Wind and Temperature up to 80 km

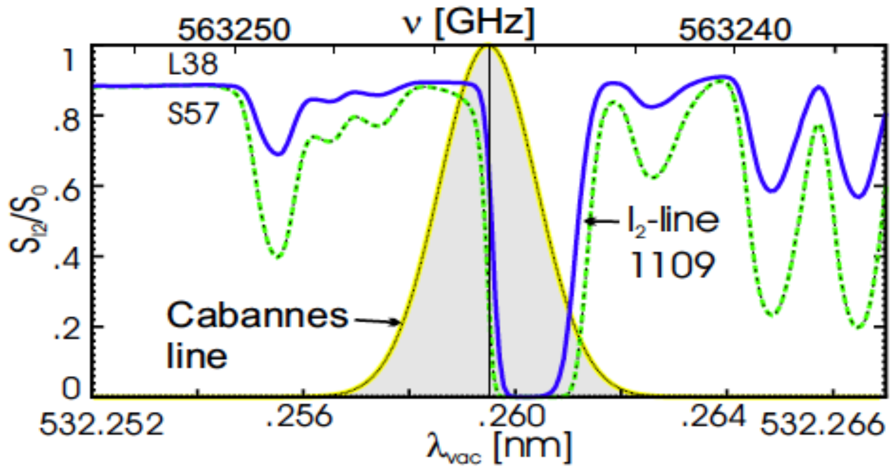

Fig. 2. Measured transmission spectrum of iodine for two cells of different length at different temperatures: 38 °C (blue L38: 15 cm long), 57 °C (green S57: 10 cm long). For reference, the Doppler broadened Cabannes line for 230 K is shown. The wavelength of the seed laser is indicated by a dotted vertical line.

Currently the data retrieval is for molecular scattering (Rayleigh) only, but since rotational and vibrational Raman as well as multiple wavelength aerosol scatterings are also detected, in principle aerosol and temperature information can be derived, so can be used to derive Doppler wind more precisely in the aerosol-loaded regions.

[Baumgarten, Atmos. Meas. Tech., 3, 1509-1518, 2010]

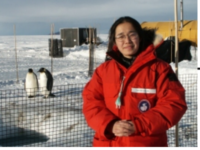

Doppler Rayleigh Iodine Spectrometer-Based Doppler Rayleigh/Mie/Raman Lidar to Profile Wind and Temperature up to 80 km

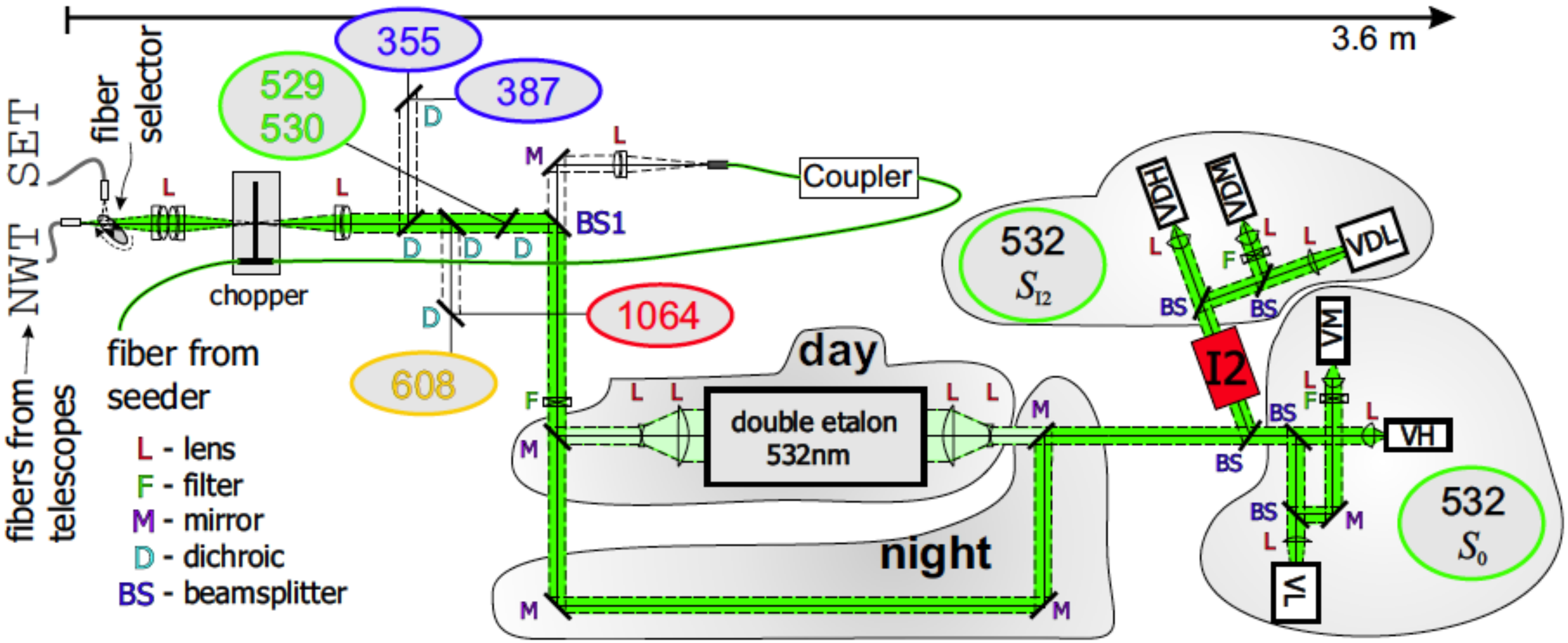

Fig. 4. Polychromatic detection system of the ALOMAR RMR lidar with emphasis on 532 nm channels. Light from the telescopes (NWT or SET) is split by wavelength and intensity. Light for the DoRIS system is detected by the channel groups 532-S_0 and 532-S_{I_2}. The system can be operated during day using a double etalon system (bandpass ∼4 pm).

[Baumgarten, Atmos. Meas. Tech., 3, 1509-1518, 2010]

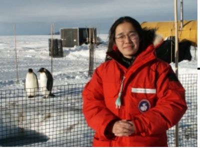

Doppler Rayleigh Iodine Spectrometer-Based Doppler Rayleigh/Mie/Raman Lidar to Profile Wind and Temperature up to 80 km

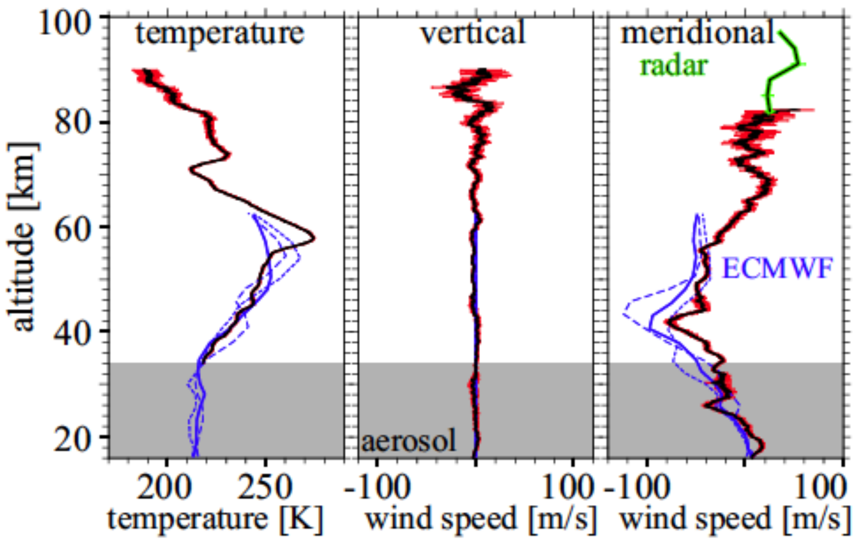

Fig. 9. Temperature, vertical and meridional wind on 17 January 2009 between 17:00 and 19:00 UT. ECMWF data from 18:00 UT (solid) and 12:00, 24:00 UT (dashed) are shown. Simultaneous observations by the collocated Meteor radar are shown. The gray area indicates altitudes with aerosol contribution as measured by the lidar.

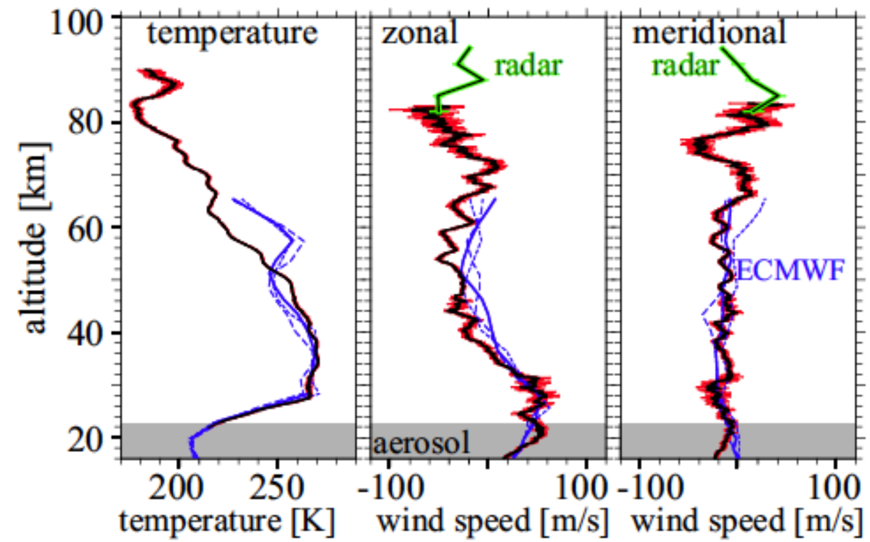

Fig. 10. Temperature and horizontal wind on 23 January 2009 between 17:00 and 19:00 UT. More details in Fig. 9.

Temperatures are derived from the integration technique combining Rayleigh and VR Raman scatterings.

$\Delta t = 2$ h, $\Delta V_{LOS} = 0.6$ m/s @ 49 km, 10 m/s @ 80 km
$P_L = 14$ W @ 532 nm, $D_{telescope} = 1.8$ m

[Baumgarten, Atmos. Meas. Tech., 3, 1509-1518, 2010]

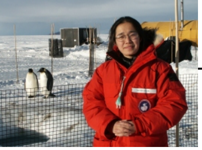

Summary

- Direct detection Doppler lidar (DDL) uses atomic/molecular absorption lines, the edge filters, or fringe-imaging techniques to discriminate or analyze the frequency or spectrum of the return lidar signals (Doppler shifted and/or broadened). Potentially, DDL can measure both wind and temperature if sufficient spectral information is provided or inquired.

- For atmospheric science study, especially for waves coupling from lower to upper atmosphere, DDLs have very high potentials for the future, especially the combination of resonance DDL in MLT region with non-resonance DDL in the troposphere, stratosphere and lower mesosphere, we may be able to profile the wind and temperature from ground all the way up to 120 km. This will be a breakthrough for atmospheric science community.

Please read our textbook Chapter 7 for direct-detection Doppler lidar and for coherent-detection Doppler lidar.